SLAC-PUB-2649
November 1980
(T/E)

POLARIZED e^-e^+ PHYSICS IN LINEAR COLLIDERS*

C. Y. Prescott
Stanford Linear Accelerator Center
Stanford University, Stanford, California 94305

ABSTRACT

Electroweak interactions at high energies are expected to be dominated by spin-dependent forces. Recent advances in the production of polarized electron beams in linear machines provide the opportunity for studying these spin-dependent effects. Polarized e^-e^+ annihilation at the Z^o pole can provide precise measurements of neutral current parameters and the best experimental challenge to the standard model of electroweak interactions.

I. INTRODUCTION

New proposals now exist in the USA and in Europe for machines which can provide high energy electron-positron collisions to investigate a regime of particle interactions dramatically different from those obtained up to the present. These new machines will permit studying the weak interactions at a strength equal to, and very likely much greater than, the familiar electromagnetic processes. The possibility of producing the intermediate vector boson, the Z^o, and studying its properties, sets the energy scale and other parameters of these machines, and provides physics objectives for the experimenters. The experimental study of the Z^o, and the interference between the photon and the Z^o, in annihilation processes should strongly challenge the gauge theory models of electroweak interactions. One of the new proposed machines is the SLAC Linear Collider (SLC) at the Stanford Linear Accelerator Center. In this talk I would like to discuss in general some of the considerations connected with Z^o physics, and specifically for this conference the interesting and important polarization phenomena expected in Z^o production in e^-e^+ annihilation. The SLAC SLC is well suited for accelerating polarized electrons to high energies, and some of the best measurements of neutral current parameters could result from polarized beam measurements in e^-e^+ annihilation at the Z^o. Although it can be argued that neutral current parameters may be measured without resorting to polarized beams, the additional information contained in the polarization studies is a powerful and practical tool for determination of the neutral current parameters. Linear machines accelerate polarized beams without loss of polarization, and techniques for producing intense polarized electron beams suitable for injection into linear accelerators have been demonstrated. These capabilities should be exploited for the studies of electroweak interactions.

II. COMMENTS ON NEUTRAL CURRENTS IN THE STANDARD MODEL

Conjectures or predictions of the existence of neutral current components in the weak interactions have existed since the late 1950's, when Zel'dovich conjectured that neutral weak currents would lead to visible effects in atomic spectra and in polarized electron scattering.[1] During the 1960's and 1970's gauge theories emerged as the basis for understanding the weak, electromag-

*Work supported by the Department of Energy, contract DE-AC03-76SF00515.

(Invited talk presented at the 1980 International Symposium on High Energy Physics with Polarized Beams and Polarized Targets, Lausanne, Switzerland, September 25 - October 1, 1980.)

netic, and strong forces.

From the development in theoretical ideas during the 1960's and 1970's, and from the experimental discoveries of the 1970's has emerged a picture of weak and electromagnetic interactions now called the standard model, based on the minimal $SU(2) \times U(1)$ gauge theory. At present no experimental evidence which bears on electroweak interactions contradicts the standard model. But the absence of experimental contradictions should not be interpreted as strong support for the present version of a standard model. The experimental data available at present do not provide precision tests of the standard model, and many predictions and fundamental concepts of the standard model are not yet seriously challenged by experiment. The experimental tools for making the precision measurements are within reach. The decade of the 1980's promises to bring into the picture precision QED-like tests of the minimal $SU(2) \times U(1)$ gauge theory the standard model is based upon. The minimal $SU(2) \times U(1)$ structure may survive or fail, but from these experimental facts will come a greatly improved understanding of these fundamental forces of nature.

Electron-positron annihilation at high energies should provide one of the cleanest tests of neutral current interactions. Electrons can annihilate on positrons with a virtual intermediate state being either a photon or a Z^o boson, according to the standard model. The diagrams which contribute are shown in Fig. 1. There is an electromagnetic piece given in lowest order by a single virtual photon exchange, and a neutral current piece, mediated by the Z^o. The two terms of Fig. 1 are indistinguishable and therefore interfere.

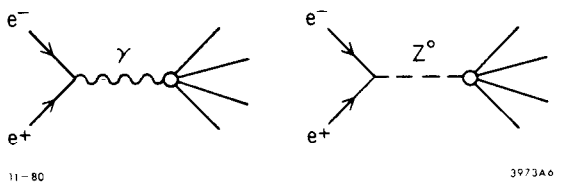

Fig. 1. Diagrams which contribute to e^-e^+ annihilation.

The standard model has four vector bosons responsible for the electroweak forces, an SU(2) triplet (W^+, W^o, W^-) and a singlet B^0. Mixing between the two neutral bosons occurs, giving the physical particles

$$\gamma = \sin\theta_w W^o + \cos\theta_w B^o \qquad (1)$$

$$Z^o = \cos\theta_w W^o - \sin\theta_w B^o \quad . \qquad (2)$$

The mixing parameter θ_w is a free parameter, not specified in the theory. Mass relations exist which depend on the value of θ_w:

$$M_W = \frac{37.3 \text{ GeV}}{\sin\theta_w} \qquad (3)$$

$$M_{Z^o} = \frac{37.3 \text{ GeV}}{\sin\theta_w \cos\theta_w} \qquad (4)$$

$$M_\gamma = 0 \quad . \qquad (5)$$

Using current values for $\sin^2\theta_w$ gives $M_W \approx 78$ GeV and $M_{Z^o} \approx 89$ GeV. Mass corrections from higher order electroweak diagrams have been calculated.[2,3] These corrections are not small; for the Z^o, an additional 3.3 GeV must be added to the value predicted in lowest order, Eq. (4), and for $W^\pm$, 3.1 GeV.

Matter consists of constituents which are the spin ½ fermions. There are the quarks which carry weak, electric and strong charge. That is, quarks couple to the heavy vector bosons W^+, W^- and Z^o, to the photon γ, and to gluons. Leptons carry no color, but do carry weak and electric charge. Neutrinos are neutral, so couple only weakly. The fermions are grouped into three generations:

$$\begin{pmatrix} u \\ d \\ \nu_e \\ e \end{pmatrix}, \quad \begin{pmatrix} c \\ s \\ \nu_\mu \\ \mu \end{pmatrix}, \text{ and } \begin{pmatrix} t \\ b \\ \nu_\tau \\ \tau \end{pmatrix} .$$

The first generation fermions are the constituents of ordinary matter. They are the lightest mass fermions and are stable. The second and third generation fermions are heavy and decay to the first generation fermions. They can only be studied in high energy processes. This organization of fermions must be regarded as a conjecture. The t quark is still "missing". There is no evidence in the PETRA data for its existence. Although it may still exist and be found in the future, its continued absence may pose a difficulty for the three generation picture.

The four bosons are responsible for the weak and electromagnetic currents. Charged current processes are mediated by W^+ and W^-. Fermions couple to the $W^\pm$ with the well-known V-A form. Through charged current interactions, quarks can change flavor. Neutral current processes are mediated by the Z^o. Fermions couple to the Z^o with a mixture of V and A couplings, but with a preference for left-handedness. Neutral currents do not change quark flavor. The electromagnetic current is mediated by the photon, γ, and couples to charged fermions with vector couplings only.

The left- and right-handed components of the fermions are treated differently in the standard model. Left-handed components are placed into SU(2) doublets:

$$\begin{pmatrix} \nu_e \\ e \end{pmatrix}_L, \quad \begin{pmatrix} \nu_\mu \\ \mu \end{pmatrix}_L, \quad \begin{pmatrix} \nu_\tau \\ \tau \end{pmatrix}_L, \quad \begin{pmatrix} \mu \\ d \end{pmatrix}_L, \quad \begin{pmatrix} c \\ s \end{pmatrix}_L, \quad \begin{pmatrix} t \\ b \end{pmatrix}_L$$

and the right-handed components remain alone in singlets,

$$e_R,\ \mu_R,\ \tau_R,\ \mu_R,\ d_R,\ c_R,\ s_R,\ t_R,\ b_R.$$

This is the minimal structure. More complicated structures such as right-handed doublets have already been ruled out by experiments for the lightest fermions e, u and d.

Each of the fundamental fermions i couples to the Z^o with couplings given by

$$g^i_{L(R)} \sim T^i_{3L(R)} - q^i \sin^2\theta_w \qquad (6)$$

where L(R) refers to the left (right) component. The quantity $T_{3L(R)}$ refers

to the third component of the weak isospin, and q^i is the electric charge. For left-handed fermions $T_{3L} = \pm\frac{1}{2}$ and for right-handed fermions, $T_{3R} = 0$. The couplings $g^i_{L(R)}$ have a strength of the order of the electromagnetic coupling e. At low energies the weak processes are suppressed relative to the electromagnetic ones due to propagator effects associated with the massive vector bosons. At asymptotic energies, however, weak and electromagnetic strengths are comparable. Equations (6) lead to a great deal of the physical phenomena associated with neutral currents. For example, parity violation in neutral current couplings arises because $g_L \neq g_R$. A beam of left-handed fermions (electrons, for example) will scatter with different probability than right-handed fermions of the same kind. Furthermore, the difference $g_R - g_L$ is large, and spin-dependent effects are correspondingly large. Asymmetries, for example, can approach unity. The fact that spin-dependent asymmetries are expected to be large has the consequence that polarization measurements can yield good measurements of neutral current couplings.

Equations (6) also imply that a universality between generations should exist. Universality means that neutral current couplings are the same for the e, μ and τ leptons and among quarks of the same charge. This prediction of universality is totally untested at present. No neutral current parameters for second or third generation fermions have been measured.

One commonly sees the neutral current parameters in the form of vector and axial vector couplings. They are simply related to those of Eq. (6) by

$$g^i_V = g^i_R + g^i_L \tag{7}$$

and

$$g^i_A = g^i_R - g^i_L \quad . \tag{8}$$

In the standard model neutral current parameters depend on a single free parameter, $\sin^2\theta_W$. It has been customary for neutral current experiments to express the results in terms of the value of $\sin^2\theta_W$. Different values of $\sin^2\theta_W$ in different processes would indicate a breakdown of the universality prediction of the standard model. For this reason precision measurements of $\sin^2\theta_W$ are desirable. At the present all measurements of $\sin^2\theta_W$ are in agreement with $\sin^2\theta_W = .232 \pm .009$.[4]

Analysis of a variety of experiments by various authors generally agrees with this value of $\sin^2\theta_W$, but the error may differ somewhat depending on various assumptions and procedures used. Figure 2 shows values of $\sin^2\theta_W$ measured in ten different processes. Two processes with the smallest reported errors, SLAC inelastic eD scattering, and the CERN CDHS inelastic neutrino scattering, are in good agreement with values $\sin^2\theta_W = .224 \pm .020$ and $.228 \pm .018$, respectively. Recent results from Mark J at PETRA report on $e^-e^+ \to \ell\bar{\ell}$ neutral current parameters. They combine $\mu^+\mu^-$ and $\tau^-\tau^+$ with e^-e^+ final states, and assuming the universality condition report the first neutral current parameters measured at a storage ring experiment.[5]

Figure 2 shows that most measurements of $\sin^2\theta_W$ at present yield large errors, and the ability to test the equality of $\sin^2\theta_W$ in different processes is poor. There are at present no precision tests of the standard model. These present measurements may continue with correspondingly reduced errors, but the true tests of the standard model will come when accelerators can produce the Z^o boson in e^-e^+ annihilations. It is probable that the best experimental tests of, and most serious challenges to, the standard model of electroweak

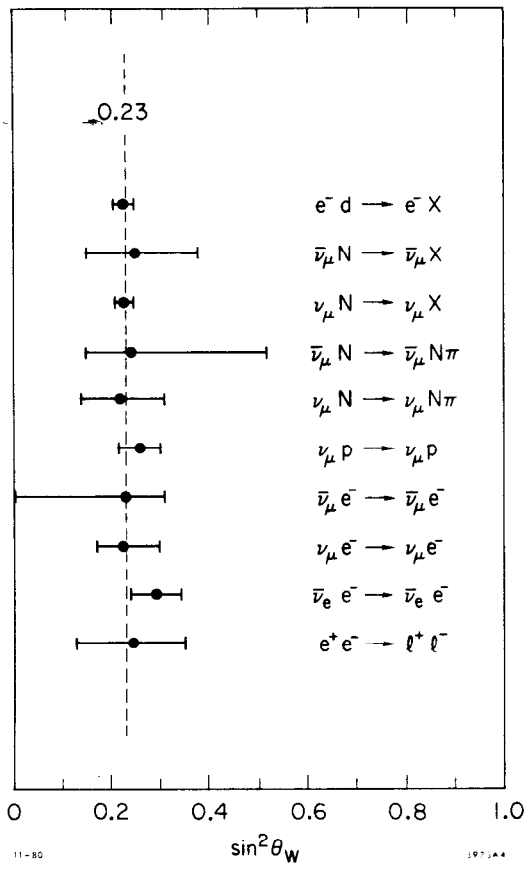

Fig. 2. Values of the parameter $\sin^2\theta_W$ obtained from various processes. The dashed line is the current weighted average .23.

interactions will come from polarized e^- beams in linear colliders in the process $e^-e^+ \to Z^o$. There are several practical reasons for this possibility. We now have means to produce intense beams of e^-_L and e^-_R. It is easy to select, or switch, from e^-_L to e^-_R, and control of the spin orientation is possible by conventional means. Many systematic errors can be virtually eliminated in measurements which are e_L versus e_R comparisons, such as asymmetries. As will be discussed later, control of the beam polarization provides control to a considerable degree of the polarization of final state particles, a technique which is extremely useful for extracting neutral current couplings. Figure 3 shows the cross section and counting rates versus center-of-mass energy, $\sqrt{s}$, for a machine which operates at a luminosity of $\mathscr{L} = 10^{30}\text{cm}^{-2}\text{sec}^{-1}$. If we take σ_{QED} to be the total cross section for $e^-e^+ \to \mu^-\mu^+$ from a single-photon exchange, and R to be the ratio $\sigma_{TOT}/\sigma_{QED}$, then low energies in e^-e^+ annihilation have a σ_{TOT} which corresponds to R ≈ 4-5. As the center-of-mass energy is raised to that of the Z^o mass, the cross section rises dramatically to a value of R ≈ 5000. The regions below and

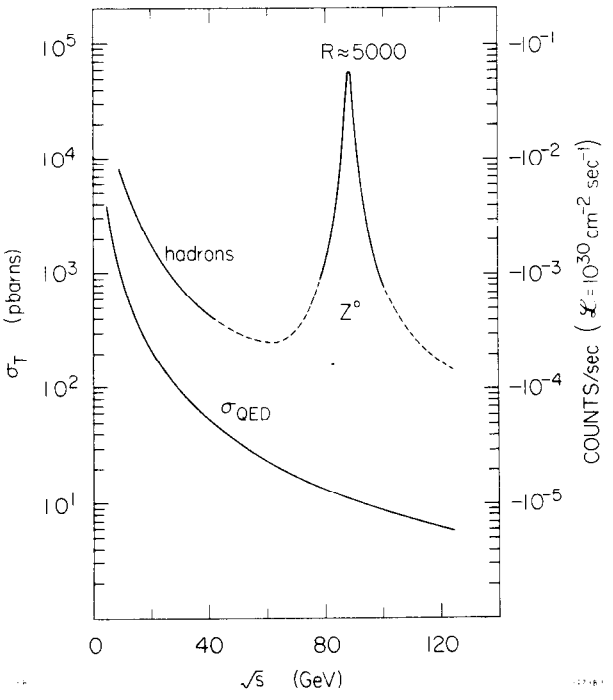

Fig. 3. Cross section for e^-e^+ annihilation versus center-of-mass energy, $\sqrt{s}$, in the standard model. σ_{QED} refers to μ-pair production from one-photon exchange only. Counting rates in a 4π detector for $\mathscr{L} = 10^{30}$ cm^{-2}sec^{-1} are shown on the right. Radiative corrections, not included here, will lower the Z^o peak and skew it to higher energies.

above the Z^o pole, where the γ and Z^o terms contribute comparable amounts to the amplitudes, can expect significant interference effects. Counting rates at the peak of the Z^o are expected to be relatively high. For a luminosity of $10^{30}cm^{-2}sec^{-1}$, several Z^o's per minute can be produced. On the other hand, at energies away from the Z^o pole, counting rates can be expected to be dismal. The precision measurements of neutral current parameters will occur only at the Z^o, and for those measurements polarization will be very useful.

III. THE SLAC LINEAR COLLIDER PROPOSAL

I would like now to describe briefly the SLAC SLC proposal in general, then look at plans to accelerate polarized electron beams in that machine. The SLAC single pass collider report is described in the Design Report.[6] The proposal is to increase the energy of the accelerator to achieve 100 GeV in center-of-mass in e^-e^+ collisions at a cost substantially below that of a comparable e^-e^+ storage ring. The primary motivation for the proposal is to build a pioneering version of linear collider machines in which two linear accelerators aim beams at each other, one beam of electrons, one beam of positrons. Intense single bunches of electrons focussed to micron size spots would collide with comparable bunches of positrons moving in the opposite direction. The SLAC linear accelerator would be upgraded to accelerate both electrons and positrons to energies up to 50 GeV. Transport lines from the end of the linac separate the bunches and transport them to a final focus and a collision point where the fundamental processes of high energy e^-e^+ annihilation can be studied. The physics motivations for studying e^-e^+ annihilation up to 100 GeV lies in the new electroweak interactions at such energies, illustrated in Fig. 3 by the strong enhancement in the cross section at the Z^o.

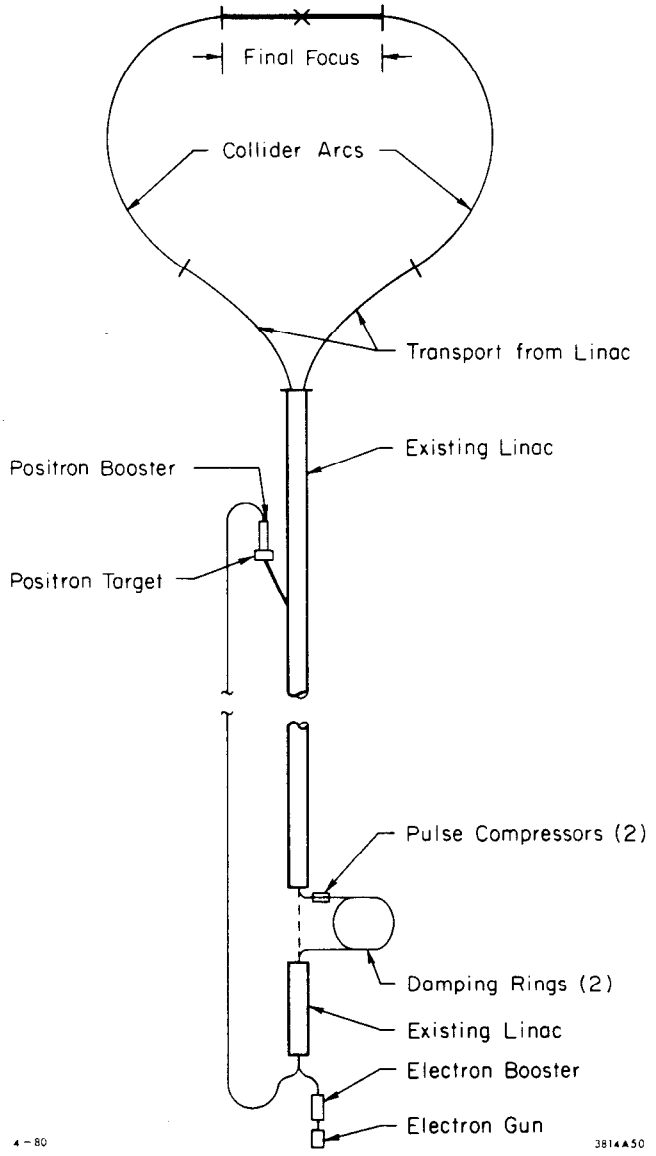

Fig. 4. Schematic layout of the SLAC single pass collider.

The general layout of the single pass collider is shown in Fig. 4. Electrons are injected into the first sections of the accelerator and boosted to 1.2 GeV energy. At this energy they are sent into a damping ring which stores them for the purpose of

reducing the transverse phase space. Exiting from the damping ring on the next machine pulse, these electrons pass through a pulse compressor, which reduces the bunch length to a millimeter in length. Two such bunches exist in the electron damping ring and are extracted for each machine pulse. The second bunch is used to generate positrons by acceleration to 33 GeV and deflection onto a target for positron production. Positrons produced are collected, transported to the front of the accelerator and accelerated to 1.2 GeV, where they are injected into their own ring for use in subsequent pulses. Electron and positron bunches are accelerated in the same machine pulse, spaced 15 meters apart. Leaving the linac, the bunches are separated into two terrain-following transport arms which bring the bunches into a final focus and collision. Table I gives a list of parameters for the single pass collider.[6]

Table I. Parameters of the single pass collider at 50 GeV (from Ref. 6)

A. Interaction Point	
Initial luminosity	10^{30} cm^{-2} sec^{-1}
Invariant emittance ($\sigma_x\sigma'_x\gamma$)	3×10^{-5} rad-m
Repetition rate	180 Hz
Beam size ($\sigma_x = \sigma_y$)	2 microns
Equivalent beta function	1 cm
B. Collider Arcs	
Average radius	300 m
Focusing structure	AG
Cell length	5 m
Betatron phase shift per cell	110°
Full magnet aperture (x;y)	10;8 mm
Vacuum requirement	$<10^{-2}$ Torr
C. Linac	
Accelerating gradient	17 MeV/m
Focusing system phase shift	360° per 100 m
Number of particles/bunch	5×10^{10}
Final energy spread	±1/2%
Bunch length (σ_z)	1 mm
D. Damping Rings	
Energy	1.21 GeV
Number of bunches	2
Damping time (transverse)	2.9 ms
Betatron tune (x;y)	7.1; 3.1
Circumference	34 m
Aperture (x;y)	±5; ±6 mm
Bend field	19.7 kg

Spin motion in the collider is relatively simple. Polarized electrons are accelerated without loss of polarization. A longitudinally polarized electron beam will enter the transport arm of the machine, and begin to precess by an amount given by the BMT equations of motion for spin.[7] For a simple transport system bending in a plane, the spin motion would be a simple g-2

precession of approximately 28 revolutions from the linac to the experimental area, at 50 GeV. However, the transport system contains vertical as well as horizontal bends to accommodate the rise and fall of the natural terrain. Spin motion will have some vertical rolling, at a somewhat slower rate than the horizontal precession. Figure 5 shows a model calculation of two spin components in the experimental area versus center-of-mass energy, for a 50% longitudinally polarized electron beam. The only component useful for physics measurements is the first one of Fig. 5, the longitudinal component. Transverse spin components for electrons which annihilate on unpolarized positrons lead to no observable effects at high energies. For longitudinally polarized e^- beams, however, one does not need to polarize the e^+ beam in order to extract the important spin-dependent parameters in the interactions. For spin-physics purposes it is sufficient to have longitudinally polarized electrons annihilating on unpolarized positrons.

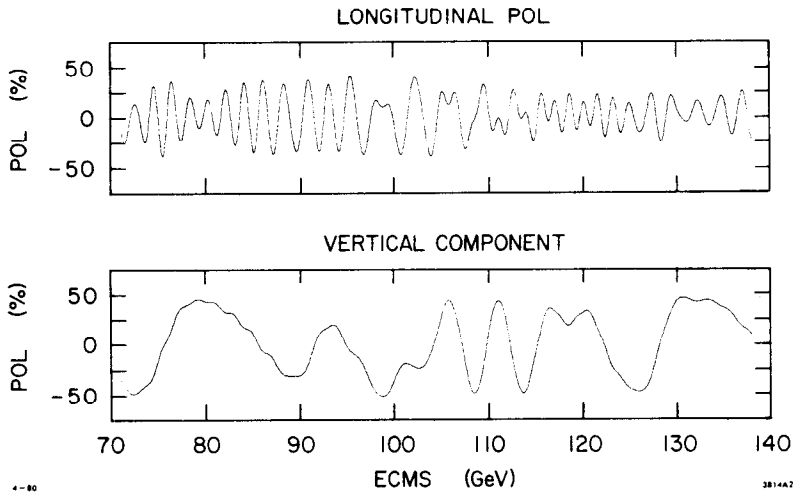

Fig. 5. A model calculation of spin components in the interaction region versus center-of-mass energy. The calculation assumes 50% polarization in the linac and includes depolarizing effects. The precession of the electron spin results in rapid oscillations of the longitudinal component and slower variations of the vertical component from a beam transport system that follows the natural terrain in the region of the north arc.

The closely spaced maxima in P_e (880 MeV apart) provide suitable points of operation for polarized beams throughout the energy range. For example, the full width of the Z^o is expected to be 2.6 GeV at half maximum, and this is large enough to contain several P_e maxima. However, plans for placing spin rotators in the injection and extraction arms of the damping ring exist.[8] Preserving spin through the damping ring requires orientating the spin transverse to the motion, parallel to the damping ring magnetic field. Figure 6 shows location of the spin rotating elements. After

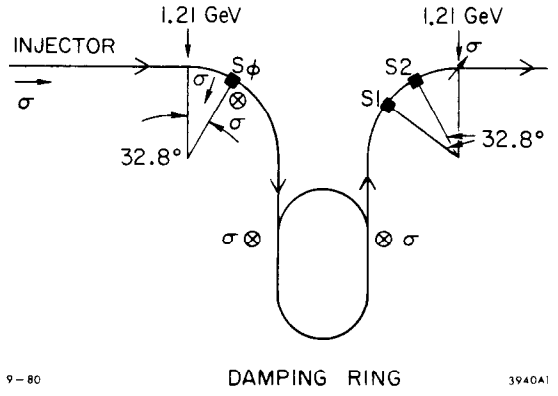

Fig. 6. Solenoids S0, S1 and S2, following 32.8° bends, rotate longitudinal spin to vertical orientation in the damping ring, then to arbitrary orientation for acceleration to high energies in the linac.

accelerating to 1.2 GeV, a horizontal bend of 32.8° followed by a solenoidal field of 6.3 Tesla-meters turns the longitudinal spin to vertical orientation. Following extraction from the damping ring, the two bends of 32.8° each followed by solenoids of 6.3 Tesla-meters in integral field path provide the freedoms to orient the spin in any arbitrary direction. The collider has the capability of providing polarized electron beams with nearly complete control of the spin degree of freedom. In the next section, some of the underlying physics of neutral currents that can be investigated with polarized beams are discussed.

IV. Z^o PRODUCTION AND DECAY FROM POLARIZED ELECTRONS

Many aspects of Z^o production in e^-e^+ annihilation have been considered in the literature. A good collection of these works, including polarization phenomena, can be found in the Les Houches summer studies[9], and earlier reports on e^-e^+ annihilation at high energies[10]. These studies concerned themselves with physics in storage ring environments, and discussions of polarization phenomena were tempered by the complexities of polarization and depolarization of beams in storage rings. At LEP where energies sufficient to produce Z^o's exist, it appears unlikely that beams will be polarized unless special measures are taken to control depolarizing effects. The potential for studying spin-dependent effects at the Z^o is apparently somewhat limited. In contrast, linear colliders can exploit fully the physics of polarized beams without introducing additional complexities. Longitudinally polarized electron beams have been accelerated at SLAC and used in several experiments. No loss of polarization has been observed. In e^-e^+ annihilation, it is not necessary to provide polarized positron beams to obtain spin-dependent effects. The reason has to do with helicity conservation at the electroweak vertex. Positive helicity electrons annihilate only on negative helicity positrons, giving +1 spin component in the beam direction. A negative helicity electron annihilates only on positive helicity positrons. If the center-of-mass energy is chosen to be the peak of the Z^o, the contribution from the single γ exchange is small. Neglecting the single photon exchange contribution, estimates of total rate of hadron production take on a simple form. The Z^o prefers left-handed particles; that is the coupling g_L is larger than g_R. The rate of production from left-handed electrons is proportional to g_L^2, and for right-handed electrons, g_R^2. If one takes P_e to be the beam polarization and $N_R(N_L)$ to be the number of incident right(left)-handed electrons, then

$$P_e = (N_R - N_L)/(N_R + N_L) \quad , \tag{9}$$

$$N_R = N_o(1 + P_e)/2$$

and

$$N_L = N_o(1 - P_e)/2 \quad , \tag{10}$$

where $N_o = N_R + N_L$. The total rate of Z^o production is given by

$$\text{Rate} \sim N_R g_R^2 + N_L g_L^2 \quad . \tag{11}$$

Using the relations defined in Eqs. (7) and (8), one finds

$$\text{Rate} \sim g_V^{e\,2} + g_A^{e\,2} + 2P_e g_V^e g_A^e \tag{12}$$

where the superscript e has been added to emphasize that electron couplings are considered. If one includes the resonance form for a Z^o of finite width Γ, then the complete expression is[11]

$$\sigma\left(e^-e^+ \to Z^o \to f\right) = \frac{e^2}{4M_Z^2 \sin^2\theta_w \cos^2\theta_w}\left(g_V^{e\,2} + g_A^{e\,2} + 2P_e g_V^e g_A^e\right)\frac{\left[2M_Z^3\Gamma_f\right]}{\left[\left(s - M_Z^2\right)^2 + M_Z^2\Gamma^2\right]} \tag{13}$$

where Γ_f is the partial width into final state f. Figure 7 shows the ratio of σ/σ_{QED} versus $\sqrt{s}$, the center-of-mass energy, near the Z^o mass. The cross section σ_{QED} is defined as $\sigma(e^-e^+ \to \mu^-\mu^+)$ from single γ exchange only. In Fig. 7, single γ exchange has been included, but is negligible near the Z^o mass. The curves are marked e_L, 0, e_R for P_e = -1,0 +1, respectively. The experimental asymmetry

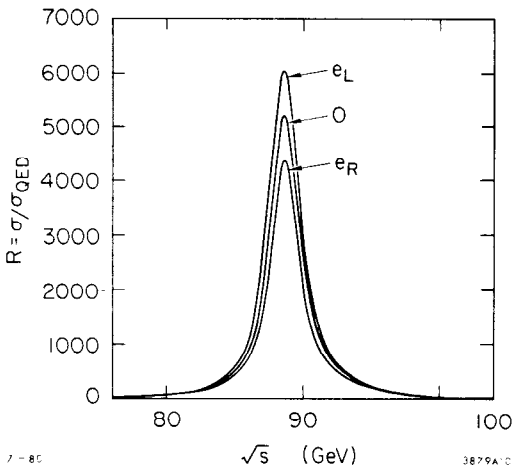

Fig. 7. $R = \sigma/\sigma_{QED}$ versus center-of-mass energy near the Z^o pole for electron beams of positive helicity (e_R), negative helicity (e_L), or unpolarized beams (0).

$$A_{exp} = (\sigma_R - \sigma_L)/(\sigma_R + \sigma_L) \tag{14}$$

where $\sigma_R(\sigma_L)$ is the total cross section for right-handed (left-handed) electrons, has the value -.16 at the Z^o peak, for $\sin^2\theta_w = .23$. In terms of the couplings

$$A_{exp} = \frac{2g_V^e g_A^e}{g_V^{e\,2} + g_A^{e\,2}} \,. \tag{15}$$

Measurement of the asymmetry, Eq. (14), and the total rate for unpolarized beams should provide a precise value for g_V^e and g_A^e, independent of other gauge theory assumptions. In particular, measurement of the total rate of production of Z^o's and the polarization asymmetry should be accurate enough to require calculation of radiative corrections (including weak vertex corrections) before meaningful comparisons between theory and experiment can be made. Figure 8a shows the present knowledge of g_V^e and g_A^e from neutrino-electron scattering. Figure 8b shows the same for $e^-e^+ \to Z^o$, estimated from statistical counting errors only. Systematic errors, which must be added to the statistical errors, will dominate at some level, but are dependent on radiative corrections and experimental details and cannot be estimated at this early date.

Z^o's produced in e^-e^+ annihilation will be polarized, even for unpolarized incident beams. The reason for this is the unequal Z^o couplings g_L and g_R. The preferential couplings to left-handed electrons give more Z^o's polarized opposite the electron beam direction than along the beam. It is straightforward to estimate the Z^o polarization. Define the polarization of the Z^o to be

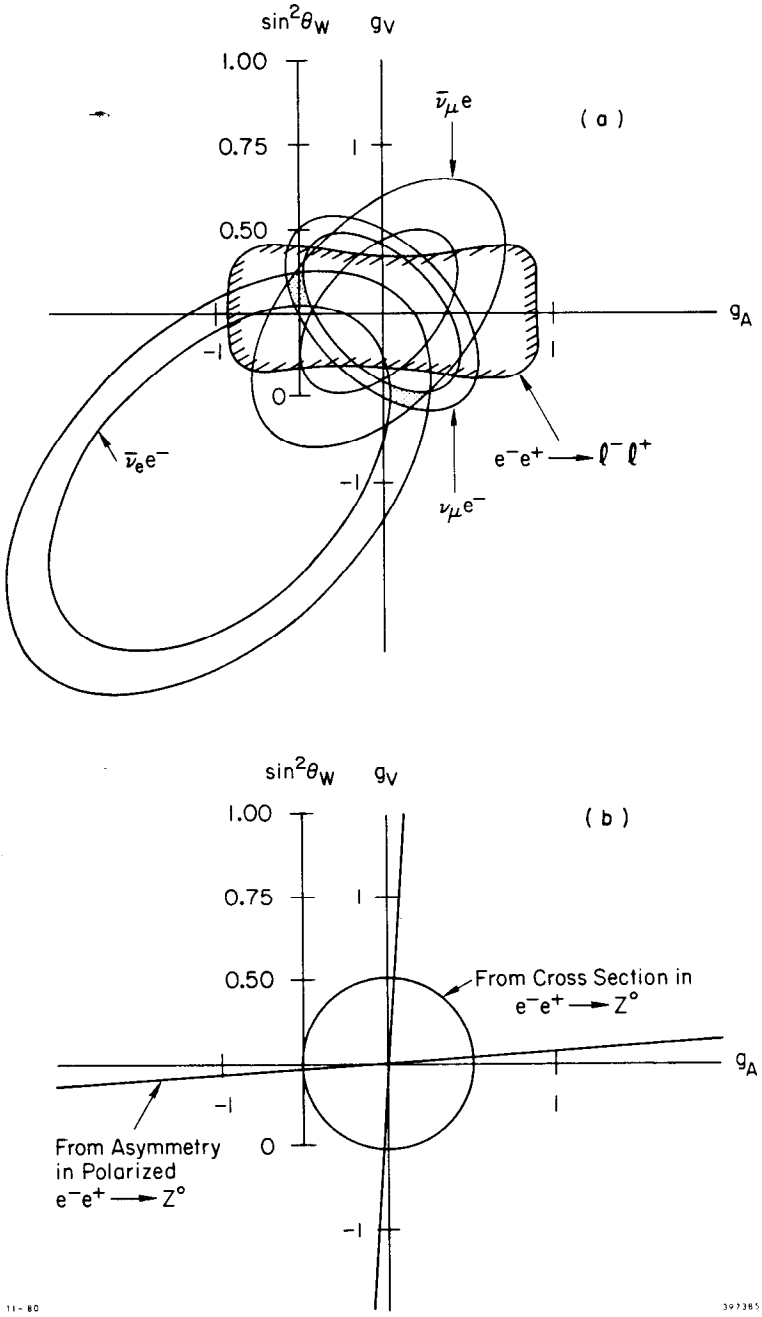

Fig. 8. Measurements of the electron neutral current parameters g_V and g_A from several processes. In (a), the present results overlap in a small region near $\sin^2\theta_W = \frac{1}{4}$. In (b), cross section values and asymmetries from $e^-e^+ \to Z^0$ will result in a circle and diagonal lines, respectively, which will greatly reduce the allowed regions in $g_A - g_V$ space. Values in (b) are for $\sin^2\theta_W = .23$. The errors for allowed regions in (b) should be dominated by systematics and are difficult to estimate, but should be considerably smaller than in (a).

$$P_Z = (N_Z^+ - N_Z^-)/(N_Z^+ + N_Z^-) \tag{16}$$

where N_Z^+ refers to spin projections ±1. Using the relations

$$N_Z^+ = (1 + P_e)g_R^2$$

and

$$N_Z^- = (1 - P_e)\, g_L^2 \tag{17}$$

and Eqs. (7) and (8), one obtains

$$P_Z = \left[2g_V^e g_A^e + P_e(g_V^{e\,2} + g_A^{e\,2})\right] / \left[(g_V^{e\,2} + g_A^{e\,2}) + 2P_e g_V^e g_A^e\right] \quad . \tag{18}$$

Figure 9 shows P_Z versus P_e for two values of $\sin^2\theta_w$, .23 and ¼. We see from this figure that Z^o's are polarized even if the beams are unpolarized, if $\sin^2\theta_w \neq$ ¼, and for polarized beams, the Z^o can be highly polarized. One would expect the alignment of Z^o spin to lead to large forward-backward asymmetries in $\mu^-\mu^+$ final states, for example. This is the neutral current analog of beta decay asymmetries from aligned nuclei.

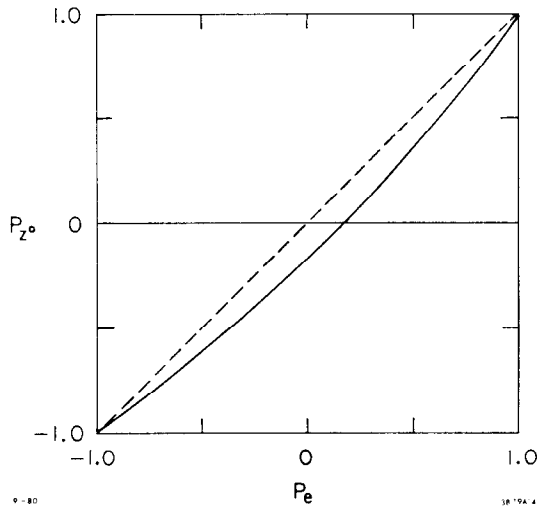

Fig. 9. Polarization of the Z^o versus incident electron beam polarization.

Forward-backward charge asymmetries are often discussed in μ pair production as a test of weak-electromagnetic interference. One also expects a charge asymmetry from polarized Z^o's. Measurement of μ pair neutral current couplings should benefit from polarized beams at the Z^o pole, relative to the more often considered weak-electromagnetic interference effects away from the pole, simply because counting rates are larger. Define the charge asymmetry to be

$$A_{ch} = \left[N(\mu^-) - N(\mu^+)\right] / \left[N(\mu^-) + N(\mu^+)\right] \quad . \tag{19}$$

If P_Z is the polarization of the Z^o, then the number of μ^-'s in the forward direction is

$$N(\mu^-) = (1 + P_Z)g_R^2 + (1 - P_Z)g_L^2$$

and

$$N(\mu^+) = (1 + P_Z)g_L^2 + (1 - P_Z)g^2 \quad . \tag{20}$$

Using Eqs. (7) and (8), one obtains

$$A_{ch} = P_Z \frac{2g_V^\mu g_A^\mu}{g_V^{\mu\,2} + g_A^{\mu\,2}} \tag{21}$$

where P_Z is given by Eq. (18). Assuming $\sin^2\theta_w = .23$ gives $A_{ch} = -.16$, .026, and +.16 for $P_e = 1$, 0, and −1, respectively. These numbers are the same for τ pairs in $Z^o \to \tau^+\tau^-$, because of the universality condition implied by Eq. (6). If one includes the single photon exchange terms, and averages over cosθ for the forward hemisphere of a 4π detector, the values are only slightly modified.

Results are shown in Fig. 10 for μ-pair of τ-pairs from e^-e^+ annihilation from e_L, 0, or e_R polarization of the incident electron beam. The Z^o pole itself is shown for reference as a dashed curve. R_μ reaches a value of 150 at the Z^o peak. The charge asymmetry is large away from the Z^o, due to γ-Z interference. The data points and associated errors are shown for two hypothetical experiments of 1000 hours each. In the first, ten 100 hour runs with unpolarized beam at a luminosity of $10^{30}cm^{-2}sec^{-1}$ are uniformly spaced below and above the Z^o at the energies shown. Each point has a statistical error on A_{ch} calculated from expected counting rates. In the second experiment, the 1000 hours is devoted to running at the Z^o pole with polarized electrons, with $P_e = \pm 50\%$. These data in each case are fit to the one free parameter, $\sin^2\theta_w$. An error on $\sin^2\theta_w$ is calculated from the statistical errors on the data points. For the unpolarized beams, an error on $\sin^2\theta_w$ of ±.0027 results, while for the polarized beam data, ±.0011 is obtained. The conclusion is that polarized beams provide a considerable enhancement of sensitivity to neutral current couplings. In reality one must include systematic errors and effects from radiative corrections, but in both cases, it is expected that polarized beams will provide better measurements relative to experiments without polarization.

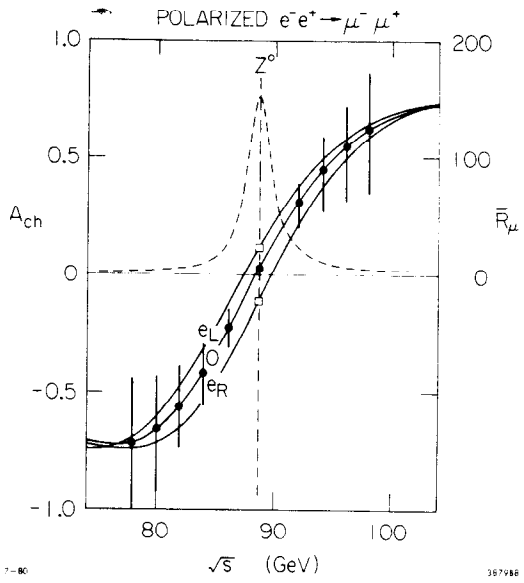

Fig. 10. The charge asymmetry for muon pairs versus center-of-mass energy for e_L, e_R and unpolarized beams. The points and associated errors compare two hypothetical experiments of 1000 hours each at $\mathscr{L} = 10^{30}cm^{-2}sec^{-1}$. Polarized beam measurements at the Z^o pole (open squares) give substantially better accuracy on muon neutral current parameters than do weak-electromagnetic interference measurements (solid dots) away from the peak of the Z^o (see text).

Charge asymmetries are expected to occur in quark pairs from Z^o decays. The Z^o decays into $\mu\bar{\mu}$, $d\bar{d}$, $c\bar{c}$, $s\bar{s}$, etc. The couplings are given by Eq. (6), and we can generalize Eq. (21) to give

$$A_{ch}^i = P_Z \frac{2g_V^i g_A^i}{\left(g_V^{i\,2} + g_A^{i\,2}\right)} \qquad (22)$$

where i refers to any fundamental fermion. Figures 11a and 11b show charge asymmetries for $\mu\bar{\mu}$ and $d\bar{d}$ pairs. As before, the single γ exchange term has been included, and cosθ has been averaged over the forward hemisphere of a 4π detector.

Measurement of the decay $Z^o \to q\bar{q}$ poses the most difficult, challenging, but important experimental problem. Quarks will materialize as jets, and flavor and charge identification in the jets may be difficult, or indeed, impossible. The degree to which quark neutral current parameters can be measured depends on how well these separations can be made. Tests of the universality relations

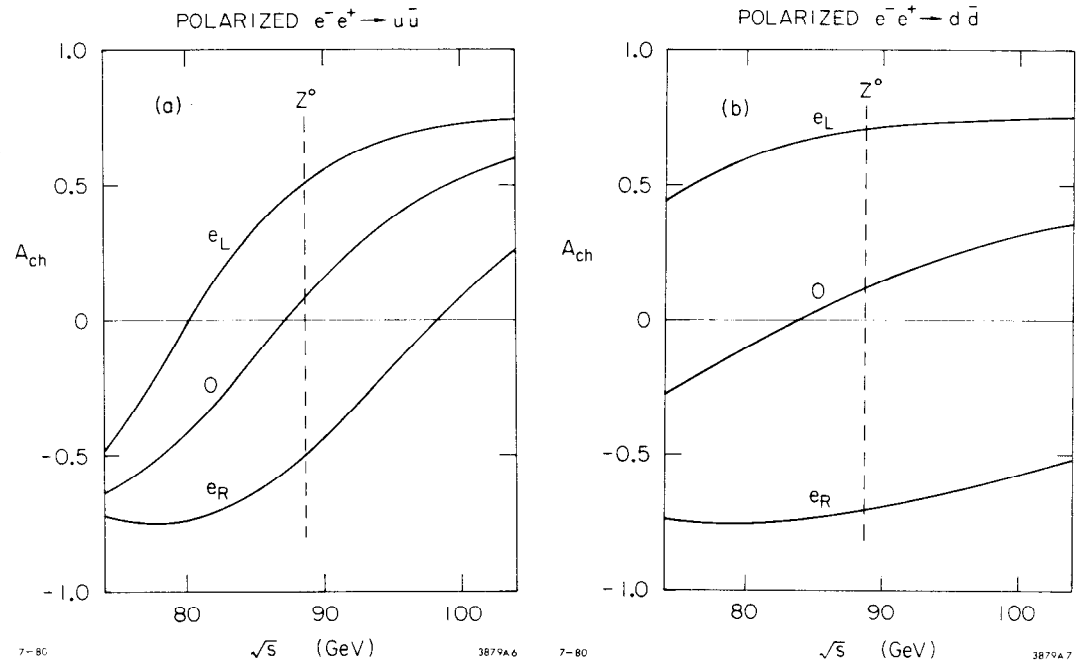

Fig. 11. Calculated charge asymmetries for $e^-e^+ \to u\bar{u}$ and $e^-e^+ \to d\bar{d}$ events.

among different generations require clean separation of quark flavors. It may be more realistic for experiments to give up on flavor discrimination and average over the jets. Tests which avoid flavor confusion may be more meaningful.

Final state leptons and quarks are expected to be polarized. It is simple to estimate the polarization of a final state fermion from $Z^o \to f\bar{f}$, if one neglects the single photon contribution. For +1 (-1) projections of the Z^o, the rate of decay in the forward direction is proportional to $g_R^2(g_L^2)$. The polarization of the fermion f is

$$\langle P_f \rangle = \frac{N_f^+ - N_f^-}{N_f^+ + N_f^-} = \frac{(1+P_Z)g_R^2 - (1-P_Z)g_L^2}{(1+P_Z)g_R^2 + (1-P_Z)g_L^2}$$

$$= \frac{2g_V^f g_A^f + P_Z(g_V^{f\,2} + g_A^{f\,2})}{(g_V^{f\,2} + g_A^{f\,2}) + P_Z(2g_V^f g_A^f)} \qquad \text{at } 0^o \quad . \tag{23}$$

For $e^-e^+ \to Z^o \to \mu^-\mu^+$ (or $\tau^-\tau^+$) the polarization is $\langle P_\mu \rangle = \pm 1$ for $P_e = \pm 1$, and $-.31$ for $P_e = 0$, for $\sin^2\theta_w = .23$, in the forward direction.

For completeness one must include the one-photon exchange contribution, and average over solid angles. Figure 12 shows the values for P_{μ^-} (or P_{τ^-}), averaging over the forward hemisphere, for a range of center-of-mass energies below and above the Z^o.

The μ^- or τ^- polarization is a respectable -31% for unpolarized beams. This polarization occurs because the Z^o prefers left-handed couplings and partially suppresses the right-handed components. This large polarization may be very useful in the case of τ's produced off Z^o's. Good measurements will result for the neutral current couplings.

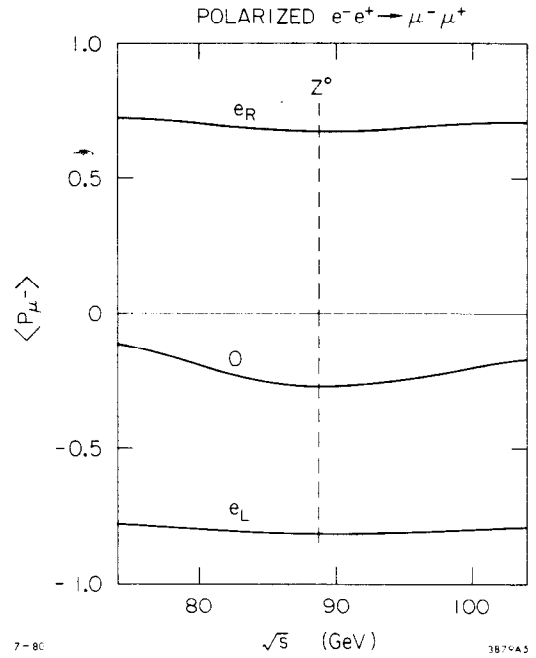

Fig. 12. Polarization of the μ^- in $e^-e^+ \to \mu^-\mu^+$ versus center-of-mass energy, for e_L, e_R and unpolarized beams.

The tau lepton has semi-leptonic and purely-leptonic decay modes. A two-body decay $\tau \to \pi\nu$ has an expected 10% branching ratio, and should be an excellent analyzer of τ spin. Tsai[12] has shown that this decay mode has an angular distribution

$$dN \sim \left(1 - h_{\pm} \cos\theta^*\right) d\cos\theta^* \qquad (24)$$

in the center-of-mass of the τ, and in the lab

$$dN \sim 1 + \langle P_Z \rangle \left[\frac{E_\pi - E/2}{E_o/2}\right] .$$

Figure 13 shows the predicted energy spectrum of the π, which is very sensitive to the incident beam polarization. Measurement of this decay mode should be clean, since identification of the τ is aided by the decay through other channels of its partner in the pair, the $\bar{\tau}$.

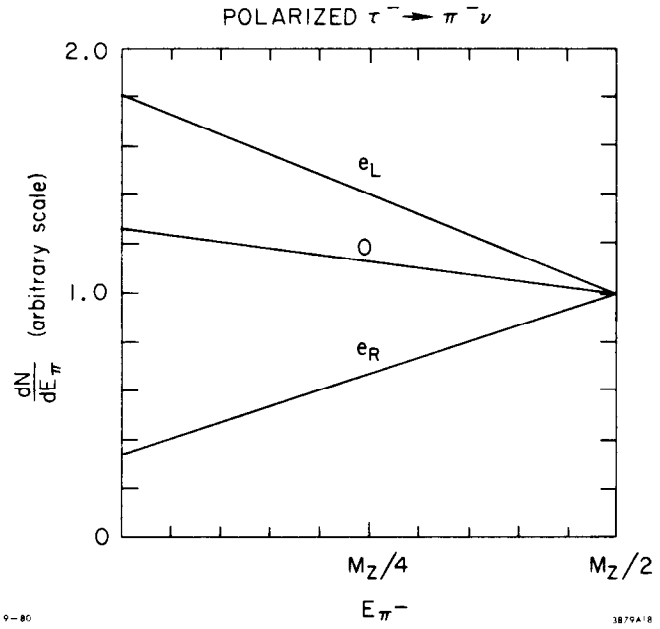

Fig. 13. The laboratory energy spectrum of pions for $\tau \to \pi\nu$ decays produced at the Z^o pole, for e_L, e_R and unpolarized beams. Measurements of the pion spectrum should provide good values of the tau polarization and its neutral current couplings.

In a sample of 10^6 Z^o's, approximately 6000 $\tau \to \rho\nu$ events should be obtained. These should yield a good measurement of $\langle P_\tau \rangle$ and through the relations similar to Eq. (20), a good value on its neutral current couplings g_V^τ and g_A^τ.

Two-body decays of the type $\tau \to \rho\nu$ are also expected to occur with a branching ratio of 23%.[13] These decays can be used to further improve measurements of the τ polarization.

Three-body decays of the tau (B.R. ~ 16% each)

$$\tau \to e\,\nu\bar{\nu} \quad \text{and} \quad \tau \to \mu\,\nu\bar{\nu}$$

likewise should teach us about tau spin and weak decays of the tau. Figure 14 shows the electron (or muon) energy spectrum assuming a standard V-A weak decay. The spectrum is significantly hardened for left-handed incident electrons. An average energy measurement of the μ or e would provide a sensitive parameter for determining the tau polarization. In a sample of 10^6 Z^o's pro-

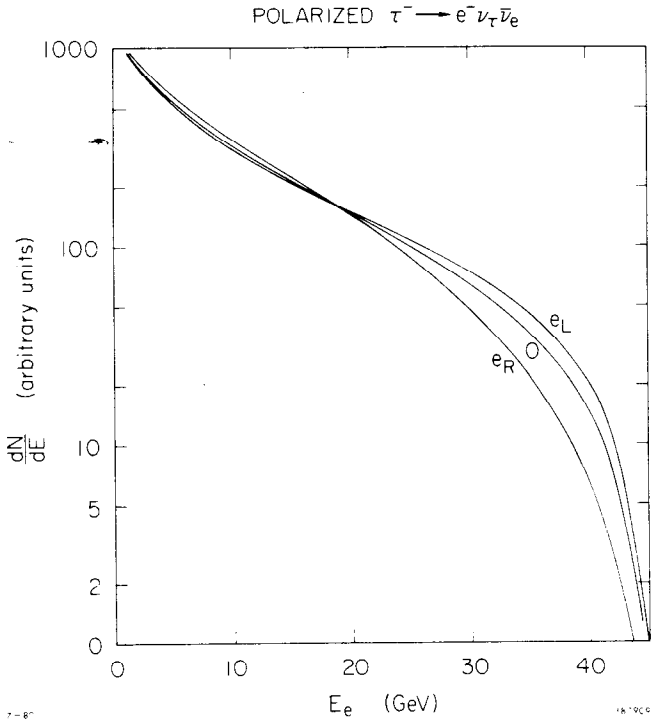

Fig. 14. The laboratory energy spectrum for electrons from $\tau^- \rightarrow e^- \nu_\tau \bar{\nu}_e$ produced at the Z^o pole from incident electrons of e_L, e_R, and 0 polarization. The mean electron energy is a good analyzer of tau polarization.

duced, approximately 20,000 decays should populate the distributions of Fig. 14, if standard model estimates remain valid. It is not unreasonable to expect 10^6 Z^o's to be produced in a reasonable length of time.

Polarization effects also extend into the hadron jets. The primary quarks have large polarizations, but QCD effects which dress the quarks may also mask these large polarizations. At the present it appears unlikely that polarization effects in hadron jets will be useful. However, this may well be proven incorrect.

In summary, neutral currents are expected to exhibit strong spin-dependent effects, and these effects are important to the experimental determination of neutral current parameters. Polarized beams greatly enhance these effects. It is not necessary to polarize the positron beam, although it is natural for this to occur in storage rings. For linear colliders, a single polarized electron beam is ideal and practical. Control of spin of electron beams has been shown to be practical in linear accelerators, and rapid reversals of spin can eliminate many sources of systematic errors. Through use of polarized beams, many neutral current parameters can be measured at the peak of the Z^o pole, with the practical advantage of providing higher counting rates than obtained away from the Z^o pole where γ-Z interference occurs. Polarization effects propagate through the Z^o into the final state. Charge asymmetries and final state polarization are important effects sensitive to incident beam polarization. Precision tests of gauge theory predictions should result from polarized beam measurements.

I wish to acknowledge contributions from several colleagues at SLAC. Charlie Sinclair, who has played a central role in bringing the laser-driven GaAs source into operation, continues the work for higher polarization. Through his efforts, the future for polarized beams in linear colliders appears bright. I would also like to thank Tom Tsao and Fred Gilman for assistance with the calculations and for numerous useful and informative discussions.

REFERENCES

1. Ya. B. Zel'dovich, JETP 33, 1531 (1957); Ya. B. Zel'dovich, JETP 9, 682 (1959).
2. M. Veltman, Phys. Lett. 91B, 95 (1980).
3. F. Antonelli et al., Phys. Lett. 91B, 90 (1980).
4. J. Kim et al., University of Pennsylvania Preprint UPR-158T (1979); P. Langacker, Proc. of Neutrino '79, Bergen, Norway, June, 1979.
5. D. Barber et al., (Mark J Collaboration), Phys. Lett. 95B, 149 (1980).
6. SLAC Linear Collider Conceptual Design Report SLAC-229 (1980); see also SLAC-PUB-2549 (1980).
7. V. Bargmann et al., Phys. Rev. Lett. 2, 435 (1959).
8. R. Steining, SLAC Note AATF/80/28 (1980).
9. Proc. of the LEP Summer Study, Les Houches and CERN, CERN Report 79-01 (1979).
10. Physics with Very High Energy e^+e^- Colliding Beams, CERN Report 76-18 (1976).
11. J. Ellis, M. K. Gaillard, CERN Report 76-18 (1976).
12. Y. S. Tsai, Phys. Rev. D4, 2821 (1971).
13. Y. S. Tsai, SLAC-PUB-2105 (1978).